Available online at www.sciencedirect.com

ScienceDirect

Physics Procedia 8 (2010) 94–103

Physics Procedia

www.elsevier.com/locate/procedia

VI Encuentro Franco-Español de Química y Física del Estado Sólido
VI[ème] Rencontre Franco-Espagnole sur la Chimie et la Physique de l'État Solide

Theoretical View on the Origin and Implications of Structural Distortions in Polyoxometalates

Xavier López*, Laia Vilà-Nadal, Xavier Aparicio-Anglès, Josep M. Poblet*

Departament de Química Física i Inorgànica, Universitat Rovira i Virgili, Marcel·li Domingo s/n, 43007 Tarragona, Spain

Abstract

Structural features of polyoxometalates (POMs) —versatile inorganic clusters of academic and technological interest— are discussed in the present article. POMs are, in general, very regular structures presenting a high symmetry in most cases. Distortions are, however, important for some electronic and magnetic properties. We herein discuss some particular geometric features that are crucial for the theoretical treatment and comprehension of well-known experimental phenomena. For instance, we have been able to understand and rationalize the geometrical distortions present in molybdenum POMs. Moreover, we can affirm that these geometrical distortions are caused by a pseudo Jahn Teller effect. In what concerns NMR chemical shifts, we present a discussion on the importance of geometry for the correct description of the signals and the key role played by the interatomic distances. Finally, a study on the adsorption of Keggin clusters on silver surfaces shows how the POM structure looses its regular shape to adapt to that new situation.

Keywords: Polyoxometalates; Distortions; NMR; Adsorption; Quantum Chemistry; DFT.

1. Introduction

The term polyoxometalate (POM) congregates a vast family of inorganic compounds built upon the aggregation of early transition metals and oxygen into close-packed clusters. Since the early XIXth century, and especially in the last fifty years, more diverse and increasingly complex POM clusters have been reported. At present, POM

* Corresponding author. Tel.: +34-977-55-9569; fax: +34-977-55-9563.
E-mail address: josepmaria.poblet@urv.cat; javier.lopez@urv.cat.

1875-3892
doi:10.1016/j.phpro.2010.10.018

compounds with high added-value have applications in fields as diverse as medicine,[i-ii] catalysis [iii-vi] or magnetism[vii-x] among many others. The development of innovative compounds and a deeper knowledge of their electronic structure has put POMs in a prominent position in the area of Inorganic Chemistry.[xi] Understanding of the chemistry governing the aggregation of the fundamental building blocks, combined with the search of more complex structures, has put POM chemistry in between the molecular and the nano worlds. Some of the structures characterized are crystals, so the structural possibilities actually range from the small Lindqvist $M_6O_{19}^{2-}$ (M = W, Mo or Nb) or the typical Keggin $XM_{12}O_{40}^{q-}$ anions (M = W, Mo and X = typically a p-block element), to the 3D packing of wheel-like POMs made of about fifty tungsten atoms each (see Figure 1). Although the synthesis and the characterization by spectroscopic methods are leading the advances in this field, Computational Chemistry has gained relevance in the last two decades, during which several theoretical research groups have published relevant data. Due to the (increasingly) large size of POM structures, together with the presence of abundant transition metal centers, computational studies are (with still rare exceptions) restricted to the application of density functional theory (DFT) methods. DFT puts together sufficient accuracy and modest calculation times, thus being the preferred tool for studying the geometry, the electronic structure and some derived properties. Among the topics that have been studied by means of DFT methods we find isomerism, protonation, reduction energies, NMR chemical shifts, encapsulation processes and electronic spectra among others.[xii] Correlated ab initio methods have also been applied for the study of magnetic properties. These methods are much more expensive than DFT ones, though more accurate, and simplifications are often introduced, such as fragment approaches to reduce the size of the system computed.[xiii-xv]

In the present paper we discuss relevant structural issues of POMs, notably concerning inherent distortions, such as the ones observed in molybdates, as well as deformations of regular structures produced by crystal packing or the environment in general and the implications these have upon the theoretical study of NMR chemical shifts. Finally, we present some preliminary results on the adsorption of a Keggin cluster on a silver surface, namely, the adsorption mode and the effects it has upon the geometry of the POM.

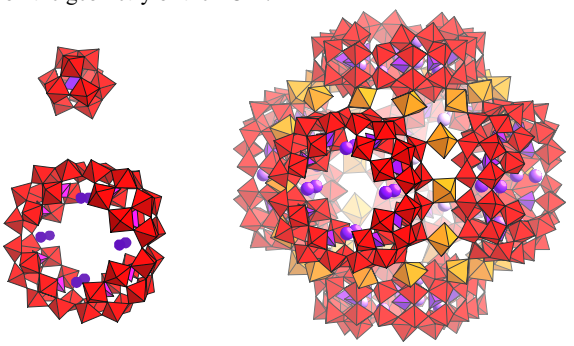

Figure 1. Increasingly complex POM structures: the $PW_{12}O_{40}$ Keggin anion (top-left), the wheel-shaped $K_8P_8W_{48}O_{184}$ cluster (bottom-left), and the basic cubic arrangement of $\{Mn_8K_8P_8W_{48}O_{184}\}_6$ wheel-shaped units that form crystals. (Color code: red octahedra are WO_6 units; purple tetrahedra are PO_4^{3-} units; orange octahedral Mn and purple sphere K^+ cations).

2. Distortions in Polyoxometalates

2.1.1. Intrinsically Distorted Polyoxometalates

POMs are metal oxide clusters that can range in size from the subnano- to the micrometer scale. For instance, the Lindqvist anion with the formula $[M_6O_{19}]^{2-}$ (in which M=Mo, W, …) has a size of < 1nm and a polyoxometalate cluster containing 368 molybdenum atoms ($\{Mo_{368}\}$ the 'Blue Lemon'), with a size of 5.4 nm –comparable to a protein– demonstrates the fascinating flexibility of POM chemistry in terms of structural complexity. The way the MO_5 and MO_6 building blocks assemble is, with few exceptions, the most regular possible, producing highly ordered aggregates that are thus very symmetrical. Consequently, only very few nonequivalent metal and oxygen

positions exist in a given compound. In the case of the α-$XM_{12}O_{40}$ Keggin anion, for example, the twelve metal sites are equivalent with T_d point group symmetry. The ideally symmetric structures of POMs are, in many cases, distorted in crystalline phase. The origin of such distortions is the close interaction with counterions, the crystal packing, the presence of solvent molecules trapped during crystallization, etc. These are sources of distortion with an origin not directly related to the structure (physical or electronic) of the POM. However, among the subclass of polyoxomolybdates, an intrinsic symmetry loss have been observed and studied. This feature, known as alternating bond length (ABL) distortion, becomes especially interesting if we stress that it is not present in polyoxotungstates. Also, an effect of such symmetry decrease is the appearance of chirality due to the loss of certain symmetry elements.

It is well known that polyoxomolybdates are more labile and flexible than their homologous tungstates, conferring to the former a higher reactivity in general. ABL distortion is, however, a quite intricate phenomenon that deserves some insight. First, it is apparently restricted to structures with interpenetrating M_nO_n ringlike motifs, as in Lindqvist (n = 4), Keggin (n = 6) and Dawson (n = 8) anions. The presence of distorted molybdate clusters featuring ABL has actually been observed for a long time[xvi-xx] but just recently explained thanks to a theoretical work.[xxi] DFT calculations driven on a set of POM structures have shown that the distorted forms get more favoured energetically than symmetrical ones as larger and more negatively charged clusters are considered. Computed values for the series $PMo_{12}O_{40}^{3-}$, $SiMo_{12}O_{40}^{4-}$ and $P_2Mo_{18}O_{62}^{6-}$ can illustrate this point. ABL distortions (d(Mo-O)$_{long}$ and d(Mo-O)$_{short}$) are shown in Table 1 for $Mo_6O_{19}^{2-}$, $XMo_{12}O_{40}^{q-}$ and $X_2Mo_{12}O_{40}^{q-}$ structures.

Table 1. Computed shortest and longest Mo–O bonds[a], for the edge-, corner-, and belt corner-sharing Mo–O–Mo bridges in Lindqvist, Keggin and Dawson polyoxomolybdates.[b]

d(Mo-O)$_{long}$ and d(Mo-O)$_{short}$	$Mo_6O_{19}^{2-}$	$PMo_{12}O_{40}^{3-}$	$S_2Mo_{18}O_{62}^{4-}$	$P_2Mo_{18}O_{62}^{6-}$
Mo–O_{edge}	1.918–1.997	1.889–2.007	1.885–2.042	1.885–2.046
Mo–O_{corner}	–	1.863–2.030	1.845–2.084	1.842–2.097
Mo–$O_{corner'}$	–	–	1.819–2.110	1.817–2.117

[a] In angstrom. [b] Lindqvist, Keggin and Dawson anions feature one, two and three types of bridging Mo-O bonds, respectively.

First, we want to stress the great agreement between experimental and computed structural parameters. Secondly, the energy difference between distorted and symmetrical is in accordance with the observed chiral properties of the anions discussed. The data demonstrate (i) that between two isostructural anions, the most charged is more distorted, and (ii) between two different anions with similar charge density, the biggest is more distorted. The responsible for the distortions observed is a pseudo-Jahn-Teller vibronic instability. The net effect upon the structure is that the expected O–Mo–O bond lengths, very similar (or equal by symmetry) in idealized structures, become O···Mo-O. This phenomenon can be viewed as a concerted migration of metal centres off the center of the MO_6 octahedron. The vibronic coupling takes place between a given vibrational normal mode and an electronic transition, giving rise to minima in the potential energy surface. So, for the species featuring ABL distortion, it exists an imaginary frequency that indicates the way into which the cluster distorts. Among the cases studied theoretically, it is worth showing that for the symmetrical (O_h) $Mo_6O_{19}^{2-}$ Lindqvist anion (the smallest POM of the series herein discussed), a normal mode analysis shows a triply degenerate imaginary frequency of 81i cm^{-1}, indicating that this structure is not a minimum. In contraposition, the octahedral $W_6O_{19}^{2-}$ structure shows an analogous normal mode at 112 cm^{-1}, which corresponds to a minimum in the potential energy surface.

An alternative point of view based on the sequence and energy of the molecular orbitals leads us to similar conclusions. The ABL distortion may be related to the energy gaps observed between frontier orbitals in molybdate structures, notably the HOMO and the LUMO. The frontier orbitals in typical symmetrical POMs have metal-oxygen nonbonding π character. From calculations it can be deduced that, upon distortion, the occupied ones get more Mo-O π bonding, and the unoccupied ones more Mo-O π antibonding, with a net stabilization of the system. Taking the undistorted structures and then comparing them to the fully distorted ones, it can be seen that smaller HOMO-LUMO gaps in undistorted forms produce larger π-orbital mixing and, thus, larger ABL distortion.

Although tungstates are virtually out of the scope of ABL distortions, the largest structures containing W_n-O_n loops can also be affected by this pseudo-Jahn-Teller phenomenon. In particular, the Preyssler tungstate $P_5W_{30}O_{110}$, with idealized D_{5h} symmetry, breaks its highest symmetry down to D_5 to get stabilized by some 10 kcal mol^{-1} upon ABL distortion. Why this polyoxotungstate and no other behave like that? Larger POMs have smaller HOMO-LUMO gaps, thus favouring π-orbital mixing. The Preyssler anion has one of the smallest HOMO-LUMO gaps in its symmetrical form among tungstates, explaining the observed concerted short-long O-W···O bonds in the equatorial region formed by $W_{10}O_{10}$ loops.

2.1.2. NMR Chemical Shifts: Significance of Structure

The performance of a nuclear magnetic resonance (NMR) analysis of the ^{183}W nucleus in a POM provides direct information on tungsten environment. Consequently is a great method for characterizing POMs both in solution and in solid state. Prediction of NMR shieldings in POMs is a challenging problem and has been a classical subject of study in the recent years. The initial DFT calculations for tungsten chemical shifts performed for small molecules, such as $[WO_{4-x}S_x]^{2-}$, $W(CO)_6$, WF_6 and WCl_6, [xxii-xxiii], lead to a roughly linear correlation between experimental and theoretical values. This results push the scientific community towards the calculation NMR chemical shifts for large POMs, despite those initial attempts were unsuccessful due to large systematic error arising from the use of basis sets with effective core potentials (ECP) [xxiv]. Later, using classical functionals such as BP86 [xxv] and Slater basis sets of TZP (or similar)[xxvi], our group established a qualitative linear correlation between calculated and experimental shifts for a great number of POMs [xxvii]. But once more the results were far to be quantitatively acceptable.[xxviii] Nevertheless precise ^{183}W NMR chemical shifts were not obtained until Bagno and co-workers [xxix-xxx] shown the need to include spin-orbit (SO) corrections at zeroth-order regular approximation (ZORA) [xxxi]and solvent effects in the calculations. Using this methodology the authors reported an average mean error of 35 ppm in a series of POMs [xxix]. It is well known that NMR chemical shifts are sensitive to very minor geometry changes. Thus, optimal geometries are necessary to accurately reproduce the experimental values.

Here we would like to prove the relevance of the optimized structure in the calculation of ^{183}W chemical shift. For this reason we will show the obtained results at several computational levels for α-$[SiW_{12}O_{40}]^{4-}$. Once determined the best approach, it is used to calculate chemical shifts for the less symmetrical anions, such as: β-$[SiW_{12}O_{40}]^{4-}$ (C_{3v}), γ-$[SiW_{12}O_{40}]^{4-}$ (C_{2v}) revealing three and four resonance lines, respectively. The structures for these anions are depicted in Figure 2.

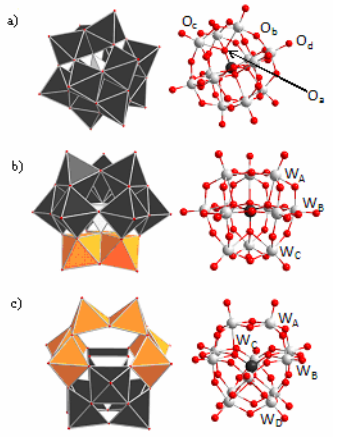

Figure 2. Polyhedra and ball-and-stick representation for several polyoxotungstates. α–$[SiW_{12}O_{40}]^{q-}$ symmetry T_d (a), β–$[SiW_{12}O_{40}]^{4-}$, C_{3v} (b) and γ–$[SiW_{12}O_{40}]^{4-}$, C_{2v} (c). Colors for the atoms (O: red, W: grey, X: black). The α–$[XW_{12}O_{40}]^{q-}$ isomer is characterized by an assembly of four edge-sharing triads W_3. Octahedra highlighted in orange show 60º-rotation of 1 and 2 triads, leading to β and γ $[XW_{12}O_{40}]^{q-}$ isomers respectively.

However, for an experimental chemist or for a spectroscopist, it may be difficult to understand why to use optimized geometries to calculate chemical shifts when for a large number of the investigated POMs there are precise and accurate experimental data from X-ray and neutron-diffraction measurements. In order to test this hypothesis we have computed the ^{183}W chemical shifts for a non-symmetrical X-ray structure of the α-Keggin SiW_{12} anion (refcode in the Cambridge Structural Database: KIDWIE, R=0.0497)[xxxii], the results are presented in Table 2.

Table 2. Calculated ^{183}W chemical shieldings for α−$[SiW_{12}O_{40}]^{4-}$ at TZP+SO+COSMO// Exp. level. $[WO_4]^{2-}$ used as a reference is computed at TZP+SO+COSMO// QZ4P+COSMO level

	σ_p	σ_d	σ_{so}	σ_{total}	δ_{cal}	δ_{exp}	$\lvert\delta_{exp}-\delta_{cal}\rvert$
$[WO_4]^{2-}$	−6944.9	9661.9	−175.8	2541.1	0	0	0
W1	−6665.7	9655.5	−206.5	2783.2	−242.1	−104	138.3
W2	−6618.1	9655.3	−207.6	2829.5	−288.4	−104	184.6
W3	−6698.7	9655.7	−210.1	2746.9	−205.8	−104	102.0
W4	−6698.6	9655.6	−209.4	2747.6	−206.5	−104	102.7
W5	−6718.1	9655.8	−208.5	2729.2	−188.1	−104	84.3
W6	−6691.3	9655.9	−208.8	2755.8	−214.7	−104	110.9
W7	−6700.3	9655.8	−212.0	2743.5	−202.3	−104	98.5
W8	−6720.0	9655.3	−210.0	2725.3	−184.2	−104	80.4
W9	−6748.9	9655.9	−209.4	2697.6	−156.4	−104	52.6
W10	−6650.9	9655.5	−210.6	2793.9	−252.8	−104	149.0
W11	−6674.5	9655.5	−209.4	2771.6	−230.5	−104	126.7
W12	−6633.9	9655.6	−208.2	2813.4	−272.3	−104	168.5
				$\overline{X}$ (δ_{cal})	−220.3	$\overline{X}$ (δ_{cal})−δ_{exp}	116.5

Along the discussion we have used the symbols TZP//TZP, TZP+SO// TZP, TZP //QZ4P, etc… For example, TZP//TZP means that NMR chemical shifts were computed with basis set TZP with the geometry optimized with the same basis set. Similarly, TZP + SO // QZ4P + COSMO means that the NMR calculations were determined with basis TZP including spin orbit corrections for the geometry optimized with basis QZ4P in aqueous solution. We have obtained twelve signals that expand in a range larger than 130 ppm (from –156 to –288 ppm) with an average value of –220 ppm. These results are very far from experimental value of –104 ppm and, as expected, they show that NMR experiments detect symmetrical structures with averaged parameters.

Once it has been determined that NMR chemical shifts are sensitive to tiny structural changes, optimal geometries are necessary to accurately reproduce experimental values. Typically, the largest discrepancies between experimental and theoretical geometries are located at terminal M=O bonds, which are computed 0.05 Å longer, in average. The geometry for the α-$[SiW_{12}O_{40}]^{4-}$ anion was optimised at several computational levels in order to check the relevance of the optimized structure in the calculation of the ^{183}W NMR chemical shifts (see Table 3). Because of the T_d symmetry of the α-Keggin anion, all tungsten atoms are identical and give a single line in the range from −177.9 to −107.9 ppm, being the experimental value −104 ppm. The best ^{183}W NMR signal is obtained at TZP+SO // TZP level, with an error $\delta_{exp}-\delta_{cal}$ of 3.9 ppm. So, the incorporation of the SO term is very important. Values when calculations incorporate the solvent effect are depicted at the three rightmost columns. In the latter case, the mean absolute error (MAE) decreases from 19.6 ppm (TZP+SO // TZP) to 9.3 ppm (TZP+SO+COSMO // QZ4P+COSMO).

Table 3 Computed chemical shifts for α-$[SiW_{12}O_{40}]^{4-}$ Keggin anion.[a]

	TZP // TZP	TZP+SO // TZP	TZP // QZ4P	TZP+SO // QZ4P	TZP // QZ4P+COSMO	TZP+SO // QZ4P+COSMO	TZP+ SO+ COSMO // QZ4P+COSMO
δ_{cal}	−157.1	−107.9	−177.9	−130.1	−163.5	−115.3	−110.1
$\lvert \delta_{exp}{}^{[b]} - \delta_{cal} \rvert$	53.1	3.9	73.9	26.1	59.5	10.3	6.1
MAE[c]	37.7	19.6	65.5	22.2	54.8	11.5	9.3

[a] Chemical shifts relative to $[WO_4]^{2-}$ computed at the same level, in ppm. [b]The experimental value of -104ppm is measured in water.[xxxiii] For this series the COSMO calculations were performed using water as solvent. [c] Mean absolute error: MAE = $\sum|\delta_{cal,i} - \delta_{exp,i}|/N$ calculated for a serie of α-$[XW_{12}O_{40}]^{q-}$ Keggin anion, where X = B, Al, Si, P, Ga, Ge, As and Zn.[xxxiv].

In conclusion, the observed ^{183}W NMR chemical shifts for the α-Keggin POM can be well reproduced if the chemical shifts are computed with a middle-sized basis set (TZP quality), incorporating the SO corrections and the solvent effect, and also using a very precise geometry obtained with a large basis set (QZ4P quality) in aqueous solution. Once a procedure to compute reasonable tungsten NMR chemical shifts for POMs is established, we applied it for the less symmetrical β- and γ-$[SiW_{12}O_{40}]^{4-}$ Keggin anions, see Table 4. Decreasing the symmetry in β-$[SiW_{12}O_{40}]^{4-}$ results in the splitting of a single line into three lines with intensity ratio (1:2:1) and also a more negative shift for all lines. The γ isomer displays four resonance lines (2:1:2:1) and, in that case, the solvent used is dimethylformamide (DMF). An analysis of the effect of the solvent on the chemical shifts can be found elsewhere [xxxiv].

As one can see in Table 4, it is worth doing the effort of optimising the geometry with an all-electron basis set of QZ4P quality. The sequence of the shifts is adequately represented by calculations with small deviations (less than 10 ppm) with respect to the experimental values.

Table 4 Observed and computed chemical shifts for several polyoxoanions

		Shift			
Anion	Atom	Calculated	Experimental	$\lvert \delta_{exp} - \delta_{cal} \rvert$	Ref.
α-$[SiW_{12}O_{40}]^{4-}$		−110.1	−104.0	6	[xxxv]
β-$[SiW_{12}O_{40}]^{4-}$	W_A	−133.3	−129.8	3.5	[xxxvi]
	W_B	−111.9	−114.5	5.4	
	W_C	−103.0	−110.0	7	
γ-$[SiW_{12}O_{40}]^{4-}$	W_A	−154.7	−160.1	5.4	[xxxvii]
	W_B	−108.1	−104.7	3.4	
	W_C	−126.6	−116.8	9.8	
	W_D	−135.8	−127.4	8.4	

As a “take-home message” we would like to emphasize that any calculation of ^{183}W chemical shifts requires a preliminary computational effort to determine very good geometries. The highly symmetric α-Keggin anion allows finding a strategy to compute precise chemical shifts. DFT geometry optimizations with a standard basis set of TZP quality provide structures that are not suitable to accurately reproduce the experimental ^{183}W NMR signals. Geometry optimizations using all electron QZ4P basis sets significantly improve the chemical shifts. We have

shown that spin–orbit corrections are also fundamental to obtain accurate shieldings for tungsten NMR chemical shifts.

3. POMs adsorbed to surfaces

From the point of view of material science, polyoxometalates (POMs) are difficult to process in order to obtain new devices. However, they are easy to combine with other materials, such as polymeric matrices or inorganic substrates.[xxxviii] This combination gives rise to compounds with interesting properties, mainly focused on catalysis. Other techniques to obtain composite materials using POMs are the fixation on metal surfaces [xxxix] or metal nanoparticles,[xl] directly or using an intermediate.

The POM–surface interaction is known to be strong, so dipping metal electrodes in POM acidic solutions suffices to prepare self-assembled POM monolayers. These monolayers are obtained not only spontaneously, but also imposing a specific potential. Several metal surfaces have been studied and compared by Gewirth and coworkers [xli-xliii] using α-Keggin polyanions. The experiments show the different behavior depending on whether gold or silver electrodes are used. Moreover, STM images were obtained,[xliv] revealing that POMs are adsorbed in a high coverage situation, as shown in Figure 3.

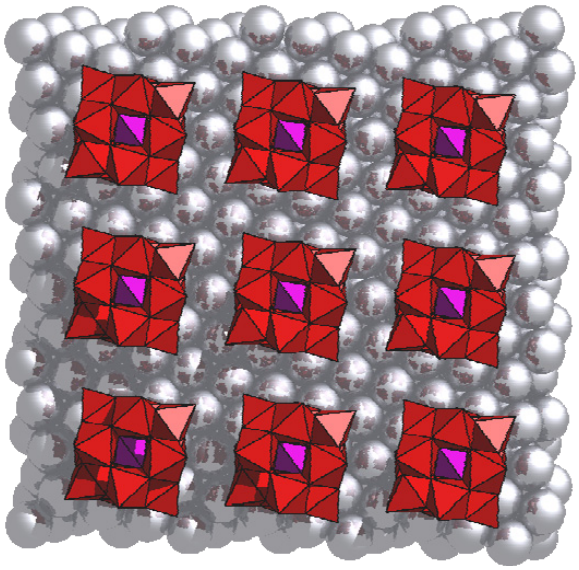

Figure 3. Representation of α-$SiW_{12}O_{40}^{4-}$ (Color code: red octahedra are WO_6 units and purple tetrahedra are PO_4^{3-} units) on Ag(111) (grey spheres) in a high coverage situation.

Here, we report preliminary results on the adsorption of α-$SiW_{12}O_{40}^{4-}$ (SiW_{12}) on Ag(111). Despite the negative charge of SiW_{12}, STM images reveal that they adsorb in a high coverage mode. Cell $\sqrt{13} \times \sqrt{13}$ R13.90° is the one used in the present calculations,[xliv-xlv] on which only the adsorption via S_4 axis of the polyoxometalate is allowed because of its size. To describe the different adsorption sites we have used the nomenclature of Gewirth,[xlvi] which defines the active site regarding the position of the heteroatom (Si) in relation to the surface. The POM decreases its symmetry from T_d to C_1 upon adsorption.

After a rather exhaustive exploration we have found that the lowest-energy system corresponds to a situation in which the Si atom is on a bridge site. Because of the POM-POM repulsion, it has been necessary to optimize the

relative disposition of the POM anions. In general, we find that the intermolecular distances between two neighboring POMs tend to maximize. In the isolated anion, the terminal tungsten-oxygen bond is usually described as a double bond whereas all the other tungsten – oxygen interactions have a single bond character. After adsorption, the terminal W-O bonds that directly interact with the surface increase their bond length from 1.71 to 1.81 Å, see Fig. 4. The adsorption via a S_4 axis also involves direct interactions between bridging oxygens and the surface, altering their bonds with the tungsten atom from values close to 1.93 Å in isolated anions [xlvii] to ~2 Å in the adsorbed anion. This elongation induces an alternating short-long bond disposition for the neighboring W-O (bridging) bonds similar to that observed in isolated molybdates (Section 2).

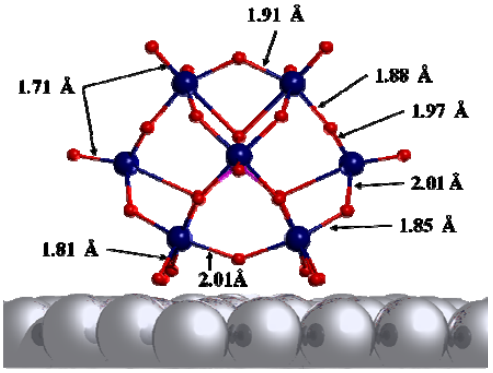

Figure 4. Selected bond distances for $[SiW_{12}O_{40}]^{4-}$ on a Ag(111) surface.

4. Conclusions

In summary, we have shown some structural features of POMs related to intrinsic distortions, NMR chemical shifts and adsorption on surfaces. POMs are regular structures with high symmetry but distortions are, however, important for some properties. We have discussed some crucial geometric features related to the theoretical treatment and comprehension of some well-known experimental phenomena. On the one hand, the intrinsic geometrical distortions present in molybdates were rationalized and assigned to a pseudo-Jahn–Teller effect. Why molybdates and not tungstates display such distortion is a key point. Also how the POM size and negative charge affect this phenomenon are interesting issues addresses in the present paper. In what concerns NMR chemical shifts, we have shown the importance of geometry for the correct description of the signals and the key role played by the interatomic distances. Geometry optimizations using all electron QZ4P basis sets significantly improve the chemical shifts. The inclusion of spin–orbit corrections is also fundamental to obtain accurate shieldings for tungsten NMR chemical shifts. Finally, a study on the adsorption of Keggin clusters on silver surfaces shows how the POM structure looses its regular shape to adapt to that new situation. As preliminary conclusions, we have demonstrated that the adsorption of SiW_{12} on Ag(111) can be studied using DFT methods combined with periodic approaches. Several sites have been optimized and analyzed. In general, it can be assumed that the adsorption induces a significant distortion of the POM indicating chemisorption on the silver surface, and therefore there is a strong interaction between the surface and POM.

References

[i] K. Dan and T. Yamase, Prevention of the Interaction Between HVEM, Herpes Virus Entry Mediator, and Gd, HSV Envelope Protein, by a Keggin Polyoxotungstate, PM-19, Biomed Pharmacother, 60(4): 169-173 (2006).
[ii] S. Shigeta, S. Mori, T. Yamase, N. Yamamoto and N. Yamamoto, Anti-RNA Virus Activity of Polyoxometalates, Biomed. Pharmacother., 60(5): 211-219 (2006).

[iii] I. V. Kozhevnikov, Catalysts for Fine Chemical Synthesis, Volume 2, Catalysis by Polyoxometalates. Wiley, Chichester (2002).
[iv] J. H. Holles, C. J. Dillon, J. A. Labinger and M. E. Davis, A substrate-versatile catalyst for the selective oxidation of light alkanes - I. Reactivity, J. Catal., 218: 42-53 (2003).
[v] K. Kamata, M. Kotani, K. Yamaguchi, S. Hikichi and N. Mizuno, Olefin epoxidation with hydrogen peroxide catalyzed by lacunary polyoxometalate $[\gamma\text{-}SiW_{10}O_{34}(H_2O)_2]^{4-}$, Chem. Eur. J., 13: 639-648 (2007).
[vi] R. Neumann and M. Dahan, A ruthenium-substituted polyoxometalate as an inorganic dioxygenase for activation of molecular oxygen, Nature, 388: 353-355 (1997).
[vii] P. Mialane, C. Duboc, J. Marrot, E. Rivière, A. Dolbeq and F. Sécheresse, Structural and magnetic properties of Mn-III and Cu-II tetranuclear azido polyoxometalate complexes: Multifrequency high-field EPR spectroscopy of Cu-4 clusters with S=1 and S=2 ground states, Chem Eur J, 12: 1950-1959 (2006).
[viii] C. Ritchie, A. Ferguson, H. Nojiri, H. N. Miras, Y. F Song, D.-L. Long, E. Burkholder, M. Murrie, P. Kögerler, E. K. Brechin and L. Cronin, Polyoxometalate-mediated self-assembly of single-molecule magnets: $\{[XW_9O_{34}]_2[(Mn_4Mn_2O_4)\text{-}Mn\text{-}III\text{-}O\text{-}II(H_2O)_4]\}^{(12-)}$, Angew Chem, Int Ed, 47: 5609-5612 (2008).
[ix] M. A. Aldaben, J. M. Clemente-Juan, E. Coronado, C. Martí-Gastaldo and A. Gaita-Ariño, Mononuclear Lanthanide Single-Molecule Magnets Based on Polyoxometalates, J Am Chem Soc, 130: 8874-8875.
[x] J. W. Zhao, J. Zhang, S. T. Zheng and G. Y. Yang, Combination between lacunary polyoxometalates and high-nuclear transition metal clusters under hydrothermal conditions: first (3,6)-connected framework constructed from sandwich-type polyoxometalate building blocks containing a novel {Cu-8} cluster, Chem Commun, 570-572 (2008).
[xi] D.-L. Long, R. Tsunashima and L. Cronin, Polyoxometalates: Building Blocks for Functional Nanoscale Systems, Angew Chem, Int Ed, 49: 1736-1758 (2010).
[xii] J. M. Poblet, X. López and C. Bo, Ab Initio and DFT Modelling of Complex Materials: Towards the Understanding of Electronic and Magnetic Properties of Polyoxometalates, Chem Soc Rev, 32(5): 297-308 (2003).
[xiii] N. Suaud, A. Gaita-Arino, J. M. Clemente-Juan and E. Coronado, Chem. Eur J., Electron delocalization and electrostatic repulsion at the origin of the strong spin coupling in mixed-valence Keggin polyoxometalates: Ab initio calculations of the one- and two-electron processes, 10(16): 4041-4053 (2004).
[xiv] N. Suaud, N. Masaro, E. Coronado, J. M. Clemente-Juan and N. Guihéry, Origin of the Paramagnetic Properties of the Mixed-Valence Polyoxometalate $[GeV_{14}O_{40}]^{8-}$ Reduced by Two Electrons: Wave Function Theory and Model Hamiltonian Calculations, Eur. J. Inorg. Chem., 34**:** 5109-5114 **(**2009).
[xv] C. de Graaf, X. López, J. L. Ramos and J. M. Poblet, Ab Initio Study of the Antiferromagnetic Coupling in the Wheel-Shaped $[Cu_{20}Cl(OH)_{24}(H_2O)_{12}(P_8W_{48}O_{184})]^{25-}$ Anion, Phys Chem Chem Phys, 12(11): 2716-2721 (2010).
[xvi] H. R. Allcock, E. C. Bissell and E. T. Shawl, Crystal And Molecular-Structure of a New Hexamolybdate-Cyclophosphazene Complex .16, Inorg Chem, 12(12): 2963-2968 (1973).
[xvii] R. Strandberg, Multicomponent Polyanions .12. Crystal-Structure of $Na_6Mo_{18}P_2O_{62}(H_2O)_{24}$, A Compound Containing Sodium-Coordinated 18-Molybdodiphosphate Anions, Acta Chem Scand, Ser A, 29(3): 350-358 (1975).
[xviii] H. D'Amour, Vergleich der Heteropolyanionen $[PMo_9O_{31}(H_2O)_3]^{3-}$, $[P_2Mo_{18}O_{62}]^{6-}$ und $[P_2W_{18}O_{62}]^{6-}$, Acta Cryst, Sect B, 32(3): 729-740 (1976).
[xix] J. F. Garvey and M. T. Pope, Chirality of Oxidized and Reduced Octadecamolybdodiphosphate Anions - Observation of a Pfeiffer Effect, Inorg Chem, 17(5): 1115-1118 (1978).
[xx] P. Souchay, R. Contant and J. M. Fruchart, Etude de la Reduction et de l'Isomerie des Acides 2-Arsenio 18-Molybdique et 2-Phospho 18-Molybdique, Hebd Seances Acad Sci, Ser C, 264(11): 976 (1967).
[xxi] L. Yan, X. López, J. J. Carbó, R. Sniatynsky, D. C. Duncan and J. M. Poblet, On the Origin of Alternating Bond Distortions and the Emergence of Chirality in Polyoxometalate Anions, J Am Chem Soc, 130(26): 8223-8233 (2008).
[xxii] A. Rodríguez-Fortea, P. Alemany, T. Ziegler, Density Functional Calculations of NMR Chemical Shifts with the Inclusion of Spin-Orbit Coupling in Tungsten and Lead Compounds, J. Phys. Chem. 103A:8288-829 (1999).
[xxiii] M. Hada, H. Kaneko, H. Nakatsuji, Relativistic study of nuclear magnetic shielding constants: tungsten hexahalides and tetraoxide, Chem. Phys. Lett. 261:7-12 (1996).
[xxiv] A. Bagno, M. Bonchio, Effective Core Potential DFT Calculations of Nuclear Shielding as a Tool for the Prediction and Assignment of the Tungsten Chemical Shift in Mono- and Polynuclear Complexes, Chem. Phys. Lett. 317:123-128 (2000).
[xxv] We applied the local density approximation featuring the Xα model with Becke's functional for exchange and the VWN parameterization with Perdew's correction for correlation. (a) A. D. Becke, Density Functional Calculations of Molecular-Bond Energies, J. Chem. Phys. 84:4524-4529 (1986). (b) A. D. Becke, A New Mixing of Hartree-Fock and Local Density-Functional Theories , J Chem Phys 98:1372-1377(1993). (c) S.H. Vosko, L. Wilk, M. Nusair, Accurate spin-dependent electron liquid correlation energies for local spin density calculations: a critical analysis, Can. J. Phys. 58:1200-1211 (1980). (d) J.P. Perdew, Density-Functional Approximation for the Correlation-Energy of the Inhomogeneous Electron-Gas, Phys. Rev. B33:8822-8824(1986).
[xxvi] NMR calculations were performed with a Slater-TZP-quality (tripe-ζ *Slater*-type orbitals plus one polarization function) basis set to describe the valence electrons. This basis set is called B1. The core electrons were kept frozen and described by single Slater functions. For a more detailed description of Slater orbitals, see Jensen, F. Introduction to Computational Chemistry; Wiley & Sons, New York (1998).

[xxvii] J. Gracia, J.M. Poblet, J. Autschbach, L.P. Kazansky, Density-Functional Calculation of the ^{183}W and ^{17}O NMR Chemical Shifts for Large Polyoxotungstates, Eur. J.Inorg. Chem. 1139-1148 (2006).
[xxviii] J. Gracia, J.M. Poblet, J.A. Fernandez, J. Autschbach, L.P. Kazansky, DFT Calculations of the 183W NMR Chemical Shifts in Reduced Polyoxotungstates, Eur. J. Inorg. Chem. 1149-1154 (2006).
[xxix] A. Bagno, M. Bonchio, J**.** Autschbach, Computational Modeling of Polyoxotungstates by Relativistic DFT Calculations of ^{183}W NMR Chemical Shifts, Chem. Eur. J. 12:8460-8471(2006).
[xxx] A. Bagno, M. Bonchio, Vicinal Tungsten–Tungsten Coupling Constants in Polyoxotungstates: DFT Calculations Challengean Empirical Rule, Angew. Chem. Int. Ed. 44:2023-2025 (2005).
[xxxi] We applied scalar relativistic corrections to them, the zeroth-order regular approximation (ZORA). (a) J. Autschbach, T. Ziegler, Nuclear spin-spin coupling constants from regular approximate relativistic density functional calculations. I. Formalism and scalar relativistic results for heavy metal compounds, J. Chem. Phys. 113:936-947(2000). (b) J. Autschbach, T. Ziegler, Nuclear spin-spin coupling constants from regular approximate relativistic density functional calculations. II. Spin-orbit coupling effects and anisotropies, J. Chem. Phys.113:9410-9418(2000).
[xxxii] J. Liu, Y. Li, E. Wang, D. Xiao, L. Fan, Z. Zhang, Y. Wang, Two novel inorganic–organic hybrids based on saturated Wells–Dawson polyoxoanion and copper–organonitrogen coordination polymer, J. Mol. Struct. 837:237-244 (2007).
[xxxiii] M.H. Alizadeh, S.P. Harmalker, Y. Jeannin, J. Martin-Frére, M.T. Pope, A heteropolyanion with fivefold molecular symmetry that contains a nonlabile encapsulated sodium ion. The structure and chemistry of $[NaP_5W_{30}O_{110}]^{14-}$, J. Am. Chem. Soc. 107:2662-2669 (1985).
[xxxiv] L. Vilà-Nadal, J.P Sarasa, A. Rodríguez-Fortea, J. Igual, L.P Kazanky, J.M Poblet, Towards the Accurate Calculation of ^{183}W Chemical Shift in Polyoxometalates: The Relevance of the Structure, Chem. Asian J. 5:97-104 (2010).
[xxxv] R. Acerete, C.F. Hammer, L.C.W. Baker, Tungsten-183 NMR of heteropoly and isopolytungstates. Explanations of chemical shifts and band assignments and theoretical considerations, J. Am. Chem. Soc. 104:5384-5390 (1982).
[xxxvi] J. Lefebvre, F. Chauveau, P. Doppelt, C. Brevard, Tungston-183 NMR spectroscopy: $^{2}J_{w\text{-}w}$ coupling. Structural application to 1-12 heteropolytungstates, J.Am.Chem. Soc. 103:4589-4591 (1981).
[xxxvii] A. Tézé, J. Canny, L. Gurban, R. Thouvenot, G. Hervé, Synthesis, Structural Characterization, and Oxidation−Reduction Behavior of the γ-Isomer of the Dodecatungstosilicate Anion, *Inorg.Chem*. 35:1001-1005 (1996).
[xxxviii] W. Qi and L.X. Wu. Polyoxometalate/polymer hybrid materials: fabrication and properties, Polym. Int. 58(11): 1217-1225 (2009).
[xxxix] M.I. Borzenko, R.R. Nazmutdinov, D.V. Glukhov, G.A. Tsirlina and M. Probst. Self-inhibition phenomena in the electroreduction of hexamolybdocobaltate(III): A combined experimental and computational study. Chem. Phys. 319(1-3): 200-209 (2005).
[xl] R. Wlodarczyk, M. Chojak, K. Miecnikowski, A. Kolary, P.J. Kulesza and R. Marassi. Electroreduction of oxygen at polyoxometallate-modified glassy carbon-supported Pt nanoparticles. J. Power Sources. 159(2): 802-809 (2006).
[xli] M.H. Ge, B.X. Zhong, W.G. Klemperer and A.A. Gewirth. Self-assembly of silicotungstate anions on silver surfaces. J. Am. Chem. Soc. 118(24): 5812-5813 (1996).
[xlii] J. Kim, L. Lee, B.K. Niece, J.X. Wang and A.A. Gewirth. Formation of ordered multilayers from polyoxometalates and silver on electrode surfaces. J. Phys. Chem. B. 108(23): 7927-7933 (2004).
[xliii] L. Lee and A.A. Gewirth. Electrochemical response of alpha-H4SiW12O40 on Ag and Au electrodes. J. Electroanal. Chem. 522(1): 11-20 (2002).
[xliv] W.G. Klemperer and C.G. Wall. Polyoxoanion chemistry moves toward the future: From solids and solutions to surfaces. Chem. Rev. 98(1): 297-306 (1998).
[xlv] L. Lee, J.X. Wang, R.R. Adzic, I.K. Robinson and A.A. Gewirth. Adsorption configuration and local ordering of silicotungstate anions on Ag(100) electrode surfaces. J. Am. Chem. Soc. 123(36): 8838-8843 (2001).
[xlvi] C.M. Teague, X. Li, M.E. Biggin, L. Lee, J. Kim and A.A. Gewirth. Vibrational spectroscopy of a Keggin polyoxometalate on metal electrode surfaces. J. Phys. Chem. B. 108(6): 1974-1985 (2004).
[xlvii] J.M. Maestre, X. López, C. Bo, J.M. Poblet and N. Casan-Pastor. Electronic and magnetic properties of alpha-keggin anions: A DFT study of $[XM_{12}O_{40}]^{n-}$ (M = W, Mo; X = Al-III, Si-IV,P-V, Fe-III, Co-II, Co-III) and $[SiM_{11}VO_{40}]^{m-}$ (M = Mo and W), J. Am. Chem. Soc. 123(16): 3749-3758 (2001).